SCIENCE CHINA
Technological Sciences

•Article•

December 2020 Vol.63 No.12: 2631–2639
https://doi.org/10.1007/s11431-020-1548-9

Performance analysis and design of self-air-cooling reciprocating compressor's cooling system

LIU YongGuang, GAO XiaoHui* & CHENG NanNan

School of Automation Science and Electrical Engineering, Beihang University, Beijing 100191, China

Received January 8, 2020; accepted February 22, 2020; published online April 24, 2020

The cooling system, as an important part of high-pressure compressor, has always been a key technical bottleneck for its miniaturization. A new type self-air-cooling system is first proposed for the reciprocating compressor through ingenious structural design without any auxiliary equipment. The transient model of cooling system is established, which regards the cooling passage as a chamber with compressibility and heat exchange considering the linear and local flow resistance. The design principle is achieved by studying the working process and key parameters characteristics, which provides the theoretical foundation for the structural design. The experimental results show that the self-air-cooling system can quickly lower the temperature of the cylinder compared with natural cooling, which has considerable theoretical significance and practical value for the miniature high pressure compressor.

self-air-cooling, reciprocating compressor, design, performance analysis

Citation: Liu Y G, Gao X H, Cheng N N. Performance analysis and design of self-air-cooling reciprocating compressor's cooling system. Sci China Tech Sci, 2020, 63: 2631–2639, https://doi.org/10.1007/s11431-020-1548-9

1 Introduction

High pressure pure air, as a high energy, secure and clean energy, is applied in the infrared guidance system and weapon precision ejection on the airplane [1–3]. How to keep producing the high pressure air on the airplane becomes very important. Multi-stage reciprocating compressor driven by swash plate becomes the research hotspot because of its compact and lightweight structure [4]. But reciprocating compressor, as a positive displacement compressor, can produce a lot of heat in the process of compressing gas [5–7]. If the heat does not dissipate in time, it will rapidly increase temperature, reduce efficiency and even cause mechanical failures [8–10]. So, the miniature and efficient cooling method become the key technique for the compressor on the airplane.

Many liquid cooling methods such as oil atomization [11], water-cooled [12], sprays cooling [13] and refrigerant injection [14] are widely applied, which even make isothermal compression possible. The air-cool compressor does not need liquid source and is convenient to move and operate [15,16]. The traditional liquid-cool and air-cool require additional auxiliary equipment. Its volume and weight are far larger than compressor itself, which can't be applied on the airplane. Some new cooling methods through improving structure have been the research focus. Professor Liu of Huazhong university of science and technology proposed a 3D-printed integrated inter cooler with complex channels, which reduces volume and weight to some extent [17]. Van et al. [18] proposed a liquid piston low-pressure compressor that not only creates near-isothermal operation, but also eliminates gas leakage and friction. Yan et al. [19] inserted the porous medium into the piston and the heat transfer surface area and power density are both increased greatly in forced cooling. Yusha et al. [20] proposed a long-stroke slow-speed reciprocating compressor to improve the heat

*Corresponding author (email: hgaoxiaohui@126.com)

dissipation. Klotsche et al. [21] developed a hollow piston reciprocating compressor and the two-phase cooling medium is contained in the hollow piston to improve heat dissipation. Mahbod et al. [22] proposed a finned reciprocating compressor whose heat transfer along one cycle has decreased by 32 times compared to a classic piston compressor. Although they have good cooling effect, they aren't suitable for the applications of high-pressure compressor through integrating multistage compression because of the complex structures.

The self-air-cooling reciprocating compressor (SACRC) is first proposed in this paper through improving the cylinder structure. The cooling system is integrated into the cylinder, which can cool the cylinder by airflow produced by itself without any auxiliary equipment. Not only it has good cooling effect and easily integrated into multi-stage compressor, but also volume and weight may be reduced. It is of great significance to the development of airborne high pressure air compressor. Therefore, performance analysis and design of the cooling system is the key to improve the cooling efficiency.

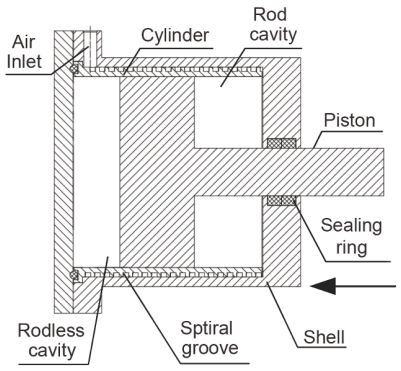

Figure 1 Mechanism of SACRC.

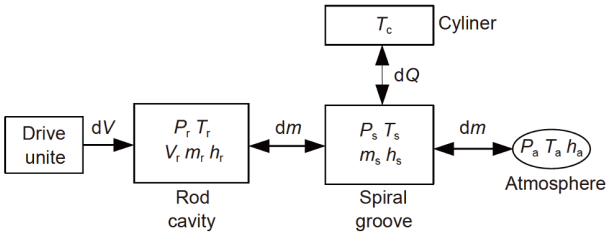

Figure 2 Cooling system.

2 Working principle

The structure of SACRC is shown in Figure 1. The cooling system is composed of rod cavity and spiral groove. The rod cavity is sealed by sealing ring. The spiral groove is machined on the outer wall of the cylinder, which forms a passage with the shell. The rod cavity is connected with the spiral groove. When the piston moves, the gas in the rodless cavity is compressed. The air is drawn in or out of the rod cavity through the spiral groove and air inlet. The airflow is formed in the spiral groove to force the convection heat exchange with the cylinder. Since the equivalent diameter of the spiral groove is much smaller than the piston diameter, the airflow's rate is high, which greatly improves the convective heat transfer coefficient. As a result, the SACRC can continuously cool the cylinder when it is working, which can make full use of the rod cavity and improve heat dissipation characteristics without auxiliary equipment.

3 Cooling system model

The compressor drives the piston periodically through the transmission mechanism. The air flows into and out of the rod cavity through spiral groove. Since the spiral groove is slender, the flow resistance is non-ignorable. So, the spiral groove can be equal to a chamber with compressibility and heat exchange. The relationship among rod cavity, spiral groove, cylinder and air is shown in Figure 2. P, T, V, m, h are respectively pressure, temperature, volume, mass and enthalpy. The subscripts r, s, a, c respectively denote rod cavity, spiral groove, atmosphere and cylinder. The rod cavity is a variable mass and volume system and its pressure and temperature are both changed under the action of drive unite. The air is periodically inhaled and discharged from the spiral groove and rod cavity. The spiral groove is a variable mass system and its pressure and temperature are both changed through heat exchange with cylinder, rod cavity and atmosphere.

The following assumptions need to be made when establishing the mathematical model:

1) The air is ideal and its characteristics are the same in working process;

2) The heat exchanging can be conducted evenly and sufficiently;

3) The kinetic energy and potential energy of air is ignored.

3.1 Drive unit model

The piston moves back and forth along sine curve driven by the crankshaft or swash plate. The stroke of the piston l is

$$l = \frac{l_p}{2} + \frac{l_p}{2}\sin\left(2\pi ft + \frac{\pi}{2}\right), \tag{1}$$

where l_p and f respectively are the motion amplitude and frequency of the piston.

The working volume of rod cavity is

$$V = l\pi(d^2 - d_r^2)/4 + V_0, \tag{2}$$

where d is cylinder inner diameter, d_r is piston rod diameter, V_0 is the clearance volume.

3.2 The first law of thermodynamics

The air in the rod cavity and spiral groove is satisfied with the first law of thermodynamics.

$$\frac{\mathrm{d}U}{\mathrm{d}t}=\frac{\mathrm{d}Q}{\mathrm{d}t}-P\frac{\mathrm{d}V}{\mathrm{d}t}+\frac{\mathrm{d}m}{\mathrm{d}t}h, \tag{3}$$

where U is internal energy, Q is heat exchange energy.

The internal energy U and enthalpy h are

$$U=mu=mc_{\mathrm{v}}T, \tag{4}$$

$$h=c_{\mathrm{p}}T, \tag{5}$$

$$R_g=c_{\mathrm{p}}-c_{\mathrm{v}}, \tag{6}$$

where c_{v} is air specific heat at constant volume, c_{p} is air specific heat at constant pressure, R_{g}=0.287 kJ/kg K is a constant.

The relationship between c_{p} and T [23] is

$$c_{\mathrm{p}}=(28.15+1.967\times10^{-3}\times T+4.801\times10^{-6}\times T^2 -1.966\times10^{-9}\times T^3)/M_{\mathrm{g}}. \tag{7}$$

3.3 Mass flow

The mass flows between spiral groove and rod cavity, atmosphere both satisfy the orifice throttle equation.

$$\frac{\mathrm{d}m}{\mathrm{d}t}=A_{\mathrm{s}}C_{\mathrm{m}}C_{\mathrm{q}}\frac{P_{\mathrm{u}}}{\sqrt{T_{\mathrm{u}}}}, \tag{8}$$

where A_{s} is the effective area of the spiral groove, C_{m} is flow parameter, C_{q} is the flow coefficient, P_{u} and T_{u} respectively are upstream absolute pressure and temperature.

When the pressure of air in the atmosphere is higher than spiral groove, the air flows from the atmosphere to the spiral groove. The mass flow from the atmosphere to the spiral groove can be achieved, which regards the atmosphere as upstream and the spiral groove as downstream. When the pressure of air in the spiral groove is higher than rod cavity, the air flows from the spiral groove to the rod cavity. The mass flow from the spiral groove to the rod cavity can be achieved, which regards the spiral groove as upstream and the rod cavity as downstream.

$$A_{\mathrm{s}}=\pi d_{\mathrm{s}}^2/4, \tag{9}$$

where d_{s} is hydraulic equivalent diameter.

The flow parameter can be written as the following for the perfect gas:

$$C_{\mathrm{m}}=\begin{cases}\sqrt{\dfrac{2\gamma}{r_0(\gamma-1)}}\sqrt{\left(\dfrac{P_{\mathrm{d}}}{P_{\mathrm{u}}}\right)^{\frac{2}{\gamma}}-\left(\dfrac{P_{\mathrm{d}}}{P_{\mathrm{u}}}\right)^{\frac{\gamma+1}{\gamma}}}, & \dfrac{P_{\mathrm{d}}}{P_{\mathrm{u}}}>P_{\mathrm{cr}}\ \text{(Subsonic)},\\ \sqrt{\dfrac{2\gamma}{r_0(\gamma+1)}}\left(\dfrac{2}{\gamma+1}\right)^{\frac{1}{(\gamma-1)}}, & \dfrac{P_{\mathrm{d}}}{P_{\mathrm{u}}}\le P_{\mathrm{cr}}\ \text{(Sonic)},\end{cases} \tag{10}$$

where γ is the specific heat ratio, r_0 is the air constant, P_{cr} is the critical pressure ratio, P_{d} is downstream absolute pressure.

$$P_{\mathrm{cr}}=\left(\frac{2}{\gamma+1}\right)^{\frac{\gamma}{\gamma-1}}, \tag{11}$$

$$\gamma=\frac{c_{\mathrm{p}}}{c_{\mathrm{v}}}. \tag{12}$$

Considering the friction in a pneumatic pipe, the equivalent flow coefficient is

$$C_q=\sqrt{\frac{d_{\mathrm{s}}}{l_{\mathrm{s}}f_{\mathrm{s}}}}, \tag{13}$$

$$l_{\mathrm{s}}=\frac{l_{\mathrm{c}}\sqrt{(\pi d_{\mathrm{sh}})^2+l_{\mathrm{h}}^2}}{l_{\mathrm{h}}}, \tag{14}$$

where f_{s} is friction factor, l_{s}, l_{h} and d_{sh} are respectively length, screw pitch and pitch diameter of the spiral groove, l_{c} is length of the cylinder.

The f_{s} depends on the Reynolds number Re and the relative roughness f_{r} of the pipe.

$$\begin{cases}f_{\mathrm{s}}=\dfrac{64}{Re}, \quad Re<80\dfrac{d_{\mathrm{s}}}{\Delta}\ \text{(laminar flow)},\\ \dfrac{1}{\sqrt{f_{\mathrm{s}}}}=-2\lg\left(\dfrac{\Delta}{3.7d_{\mathrm{s}}}+\dfrac{2.51}{Re\sqrt{f_{\mathrm{s}}}}\right),\\ \qquad 80\dfrac{d_{\mathrm{s}}}{\Delta}<Re<4160\left(\dfrac{d_{\mathrm{s}}}{\Delta}\right)^{0.85}\ \text{(transition)},\\ f_{\mathrm{s}}=\dfrac{1}{\left[2\lg\left(\dfrac{d_{\mathrm{s}}}{2\Delta}\right)+1.74\right]^2},\\ \qquad Re>4160\left(\dfrac{d_{\mathrm{s}}}{\Delta}\right)^{0.85}\ \text{(turbulence)},\end{cases} \tag{15}$$

where Δ=45 μm is absolute roughness of the spiral groove.

$$Re=\frac{4\left|\dfrac{\mathrm{d}m}{\mathrm{d}t}\right|}{\pi\mu d_{\mathrm{s}}}, \tag{16}$$

$$\mu=\mu_0\left(\frac{T}{288.15}\right)^{1.5}\frac{288.15+B}{T+B}, \tag{17}$$

where μ is the air dynamic viscosity, μ_0=1.7894×10^{-5} N s/m^2 is the dynamic viscosity at 288.15 K (15°C), B=110.4 K is a constant.

3.4 Heat exchange

The convective heat transfer occurs between the cylinder and air in the spiral groove and the exchange heat energy Q between them is

$$Q=c_sh_s\pi\mathrm{d}_sl_s(T_{\mathrm{c}}-T_{\mathrm{s}}), \tag{18}$$

where c_{s} is the helical tube correction factor [24], h_{s} is the convective exchange coefficient between cylinder and air in the spiral groove, T_{c} is the cylinder temperature.

$$c_{\mathrm{s}}=1+3.54\frac{d_{\mathrm{s}}}{d_{\mathrm{c}}}, \tag{19}$$

$$h_s = \frac{Nu\lambda_s}{d_s}, \tag{20}$$

where λ_s, Nu_s are respectively the heat conductivity coefficient and Nusselt number of the air in the spiral groove.

When the air pressure is between 100 Pa and 1 MPa, λ_s is only related to temperature.

$$\lambda_s = \lambda_0\left(\frac{T}{273.15}\right)^{0.8}, \tag{21}$$

where λ_0=2.44×10^{-2} W/m K is the air heat conductivity coefficient at 273.15 K.

When the air is respectively in laminar flow, transition and turbulence, Nu are

$$\begin{cases} Nu_{\text{lam}} = 1.86(Re\cdot Pr)^2\left(\dfrac{\mu}{\mu_c}\right)^{0.14}, \\ \qquad Re < 80\dfrac{d_s}{\Delta}\ \text{(laminar flow)}, \\ \dfrac{1}{2}\left[(1-k_{Nu})Nu_{\text{lam}} + (1+k_{Nu})Nu_{\text{tur}}\right], \\ \qquad 80\dfrac{d_s}{\Delta} < Re < 4160\left(\dfrac{d_s}{\Delta}\right)^{0.85}\ \text{(transition)}, \\ Nu_{\text{tur}} = 0.027Re^{0.8}Pr^{1/3}\left(\dfrac{\mu}{\mu_c}\right)^{0.14}, \\ \qquad Re > 4160\left(\dfrac{d_s}{\Delta}\right)^{0.85}\ \text{(turbulence)}, \end{cases} \tag{22}$$

$$k_{Nu} = \tanh\left(8\frac{Re-80\dfrac{d_s}{\Delta}}{4160\left(\dfrac{d_s}{\Delta}\right)^{0.85}-80\dfrac{d_s}{\Delta}}-4\right), \tag{23}$$

where μ_c is the air dynamic viscosity in the temperature T_c.

$$Pr = \frac{\mu c_p}{\lambda_s}, \tag{24}$$

When the heat exchange between the air and cylinder is Q, the cylinder temperature difference ΔT is

$$\Delta T = Q / C_c m_c, \tag{25}$$

where C_c=480 J/kg K is the specific heat capacity of the cylinder material, m_c is the cylinder mass.

The mathematical models of the spiral groove and rod cavity respectively are firstly established based on the first law of thermodynamics, mass flow equation and heat exchange.

The SACRC's cooling system's model is achieved through connecting spiral groove and rod cavity considering their mass and energy exchange

4 Analysis of cooling system

When the compressor woks, the cylinder can be heated by the compressed gas, which reduces the inspiratory efficiency. So, the efficiency of the compressor is inversely proportional to the cylinder temperature.

In order to analyze performance of the cooling system, the initial temperature of the cylinder is set to a constant. When the initial conditions are T_c=50°C, P_a=1.013 bar, T_a=20°C, the cooling system's air performance in one period is shown in Figure 3. When the piston moves in the direction of the arrow (Figure 1), the air is inhaled into the rod cavity through the spiral groove. With the piston speed increasing, the performance of the cooling system is as follows.

1) The suction mass flow goes up (Figure 3(a)) and the convective exchange coefficient increases rapidly after a low initial value (Figure 3(b)). This indicates that the air in the spiral groove is from laminar flow to turbulence and the increase of airflow rate is very important for convective exchange coefficient.

2) The pressure of the air in the rod cavity and spiral groove decrease because of increasing flow resistance (Figure 3(c)). The air temperature decreases based on the thermal power conversion principle.

3) The temperature of the air in the rod cavity decreases rapidly after transient elevation (Figure 3(d)). The air in the spiral groove is hotter than rod cavity at the beginning of suction because of absorbing heat from the cylinder.

4) The temperature of the air in the spiral groove rapidly decreases in the initial stage (Figure 3(d)) because of inhaling cold air, heat-work conversion and low convective exchange coefficient. And then, the temperature rises because of the rapidly increasing convective exchange coefficient. So, the heat exchange between cylinder and air in the spiral groove gradually increase (Figure 3(e)).

The effect is opposite with piston speed decreasing. When the piston is moving in the opposite direction of the arrow (Figure 1), the air is compressed and discharged out of the rod cavity through the spiral groove. Therefore, the pressure of the air in the rod cavity and spiral groove is higher than P_a (Figure 3(c)). The air temperature maybe higher than cylinder (Figure 3(d)) and the heat is transferred from cylinder to the air. But the air in the spiral groove absorbs more heat from the cylinder than it emits in one period (Figure 3(e)). Thus, the cylinder temperature rapidly drops first and then slowly rises in one period and its overall trend is falling (Figure 4). The cylinder is cooled under the action of its own cooling system.

5 Research on the characteristics of key parameters

It can be seen that the cooling system performance is mainly related to the flow resistance. If it is higher, the suction pressure and temperature are both lower and the air can absorb more heat from cylinder. But the exhaust pressure and

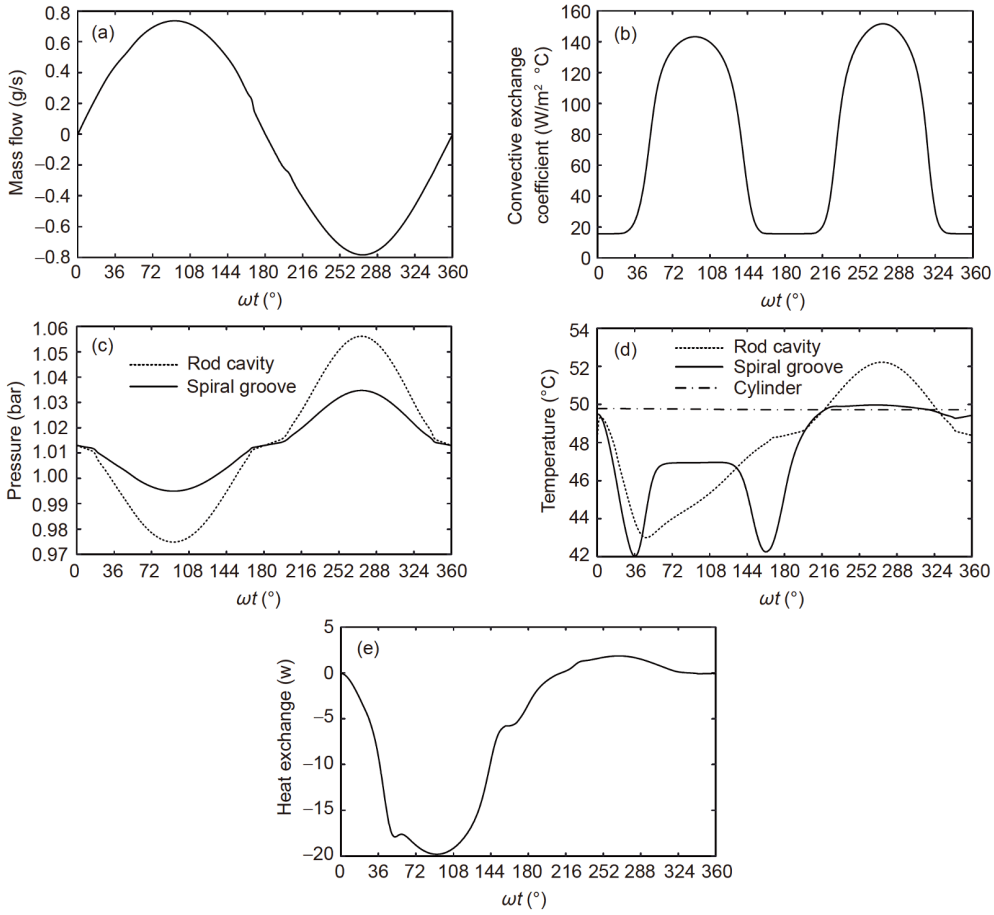

Figure 3 Cooling system performance in one period. (a) Mass flow; (b) convective exchange coefficient; (c) pressure; (d) temperature; (e) heat exchange.

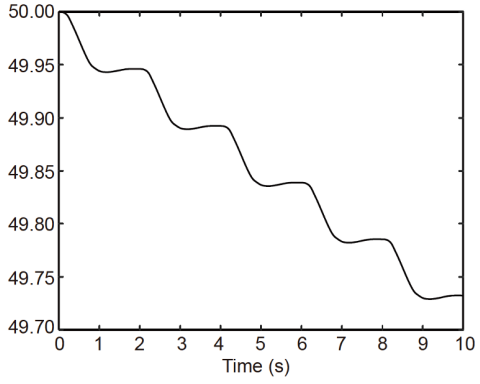

Figure 4 Cylinder temperature.

temperature are both higher and the cylinder may transfer heat to the air. The flow resistance is mainly related to hydraulic equivalent diameter and frequency according the cooling system model. The relationships between structural parameters meet the following requirements. When d=100 mm and d_r=25 mm, the key parameters characteristics are studied.

$$d_c = d + d_s + 5\,\text{mm}, \tag{26}$$

$$l_h = d_s + 3\,\text{mm}, \tag{27}$$

$$l_c = l_p + 20\,\text{mm}. \tag{28}$$

5.1 Hydraulic equivalent diameter of spiral groove

The cooling system performance curves are shown in Figure 5 at different hydraulic equivalent diameters. When d_s is small, the airflow rate and flow resistance become big and the air pressure and convective exchange coefficient are both higher (Figure 5(a) and (b)). The good heat exchange raises the air temperature in the suction (Figure 5(c) and (d)). But the compression in the exhaust produces more heat, which increases the air temperature and even transfers heat back to the cylinder. Although the higher convective exchange coefficient can improve the heat exchange, the compression produces more heat, which can reduce the cooling effect. When d_s is big, although the heat exchange is worse, the compression produces less heat. So, the optimum hydraulic equivalent diameter can improve the cooling system performance.

The cylinder temperature curve is shown in Figure 6 at different d_s in a minute. The cylinder temperature decreases

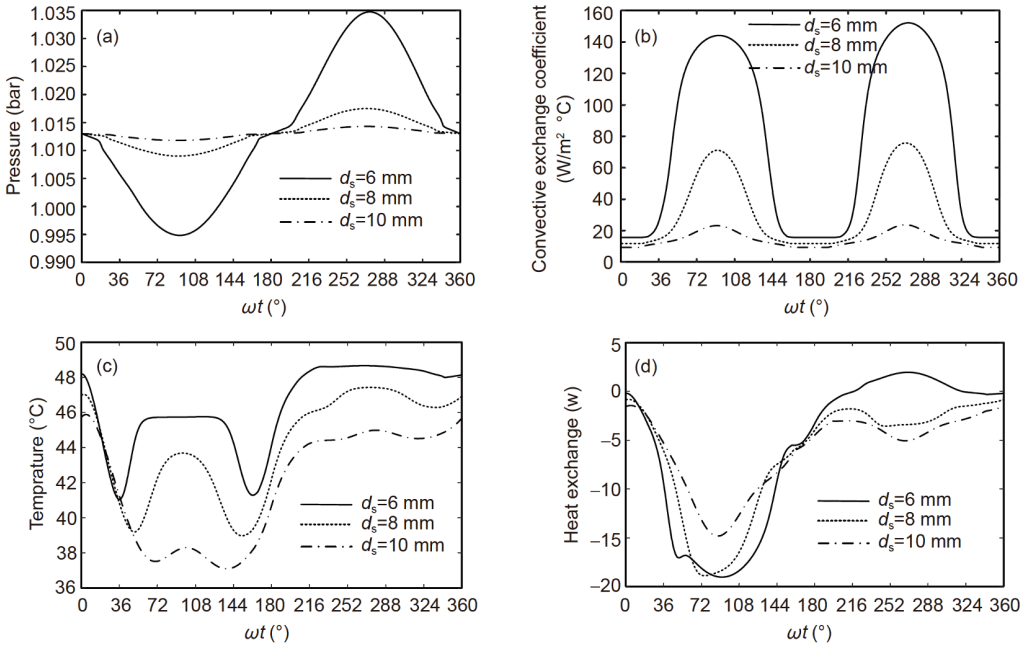

Figure 5 Different hydraulic equivalent diameters. (a) Pressure; (b) convective exchange coefficient; (c) temperature; (d) heat exchange.

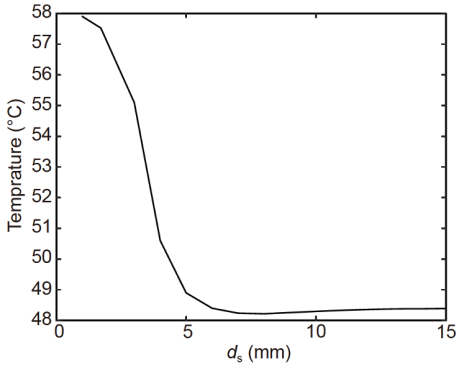

Figure 6 Cylinder temperature at different d_s.

rapidly at first and increases subsequently with increasing ds. The larger or smaller d_s can both reduce cooling effect. When d_s is small, it is sensitive to the cooling effect. But the lager d_s is relatively insensitive although it can also reduce the cooling effect.

5.2 Frequency

The cooling system performance curves in one period are shown in Figure 7 at different frequencies. When f is high, the airflow rate and flow resistance become big and the air pressure and convective exchange coefficient are both higher (Figure 7(a) and (b)). The good heat exchange raises the air temperature in the suction (Figure 7(c) and (d)). But the compression in the exhaust produces more heat, which increases the air temperature and even transfers heat back to the cylinder. Although the higher convective exchange coefficient can improve the heat exchange, the compression produces more heat, which can reduce the cooling effect.

The cylinder temperature curves are shown in Figure 8 at different frequencies. When the compressor works in the same periods, the cooling effect becomes worse with increasing frequencies. While it gets better first and then worse in the same working hours. Although the cooling effect in one period is good at low frequency, the total heat loss is low because of fewer number of cycles. So, the optimum frequency is selected according to the specific conditions.

The relationship between frequency and optimum d_s is shown in (Figure 9). The optimum d_s is larger with the increasing frequency. It is sensitive at low frequency and roughly linear at high frequency.

5.3 Length-to-diameter ratio

The cooling system performance curves in one period are shown in (Figure 10) at different length-to-diameter ratios under the same V. When l_p/d is large, the compressor is slender and the lengthen of spiral groove l_s is long. The flow resistance becomes big and the air pressure increases (Figure 10(a)). Although their convective exchange coefficients have no obvious difference because of the same volume (Figure 10(b)), the longer l_p can increase heat exchange and temperature in the suction (Figure 10(c) and (d)). But the more heat can be produced because of high flow resistance in the exhaust, which increases the temperature and reduces heat exchange. When l_p/d is small, there is less heat exchange in the suction and more in the exhaust.

The cylinder temperature curve is shown in (Figure 11) at

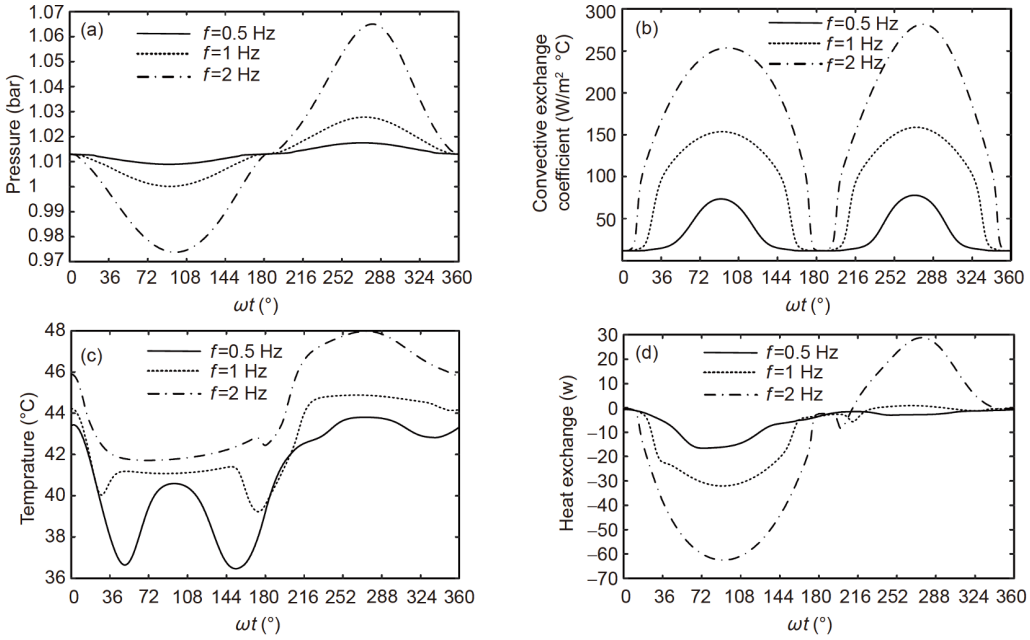

Figure 7 Different frequencies. (a) Pressure; (b) convective exchange coefficient; (c) temperature; (d) heat exchange.

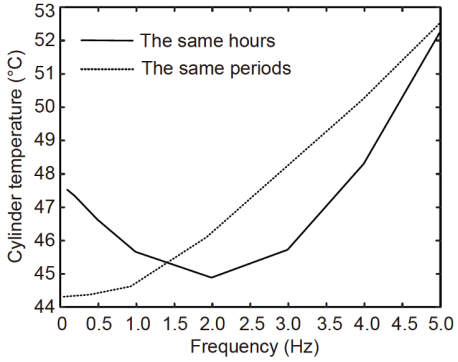

Figure 8 Cylinder temperature at different frequencies.

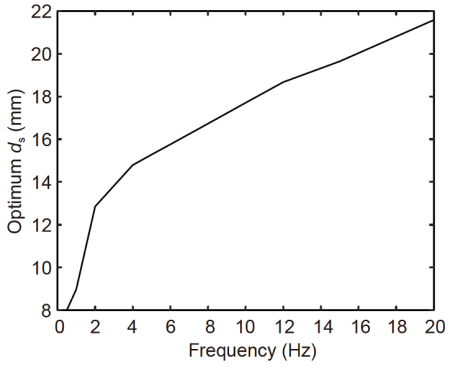

Figure 9 Optimum d_s.

different l_p/d in a minute. The cylinder temperature decreases rapidly at first and increases subsequently with increasing l_p/d. The larger or smaller l_p/d can reduce cooling effect. It is insensitive as the maximum temperature difference is only 0.31°C when l_p/d is from 0.1 to 6.

6 Experimental research

The SACRC testbed is shown in Figure 12, which is composed of controller, motor, leading screw, piston, cylinder, pressure sensor, temperature sensor, and data acquisition. The motor drives the piston along the sine through leading screw to compress air. The Smaq USB-3110 is used as data acquisition to collect pressure and temperature of the air in the rod cavity. The sample rate is 100 Hz. The structural parameters of the SACRC: d=100 mm; d_r=25 mm; d_s=8 mm; l_p=50 mm. When the cylinder is heated to 50°C, the piston is driven by motor at 0.5 and 2 Hz and works one minute, the pressure and temperature of the air in the rod cavity are shown in Figure 13, which shows that the simulation curves agree well with the test results. The temperature curves of the cylinder are shown in Figure 14 under natural cooling and compulsory cooling at 2 and 0.5 Hz. The cylinder temperatures are respectively 48°C, 47.3°C and 46.5°C after a minute and fall 2°C, 2.7°C and 3.5°C. The temperature drop rate of forced cooling at 2 Hz is 1.5 times to the natural cooling, which shows that the self-air-cooling system has good cooling performance.

7 Conclusions

(1) The self-air-cooling system can quickly lower the temperature of the cylinder without any auxiliary equipment,

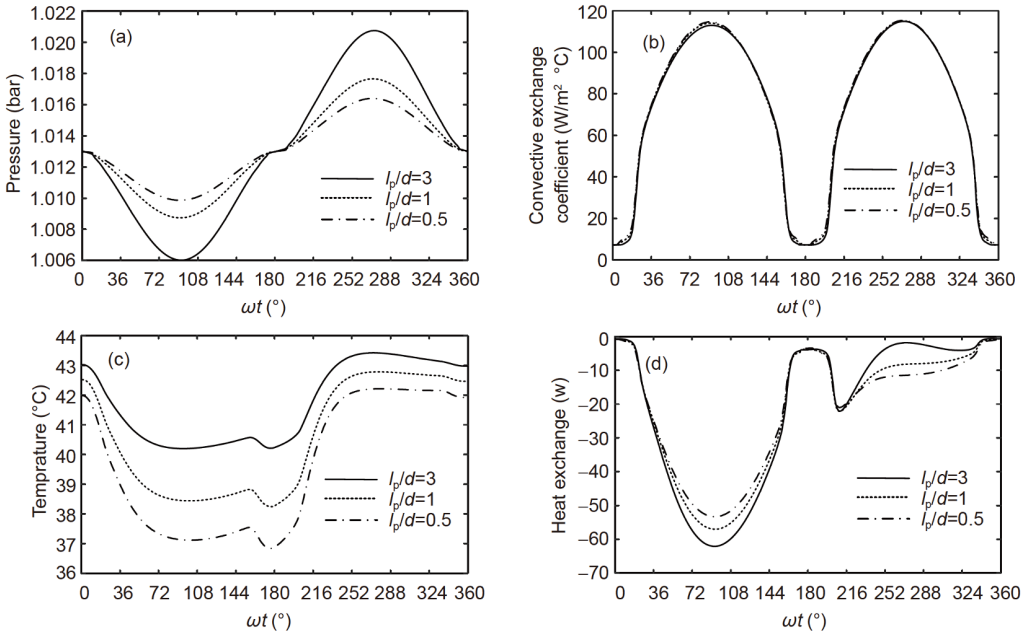

Figure 10 Different length-to-diameter ratios. (a) Pressure; (b) convective exchange coefficient; (c) temperature; (d) heat exchange.

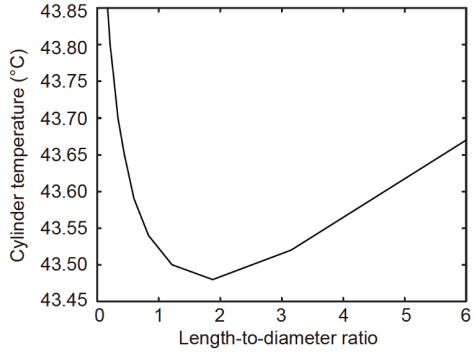

Figure 11 Cylinder temperature at different l_p/d.

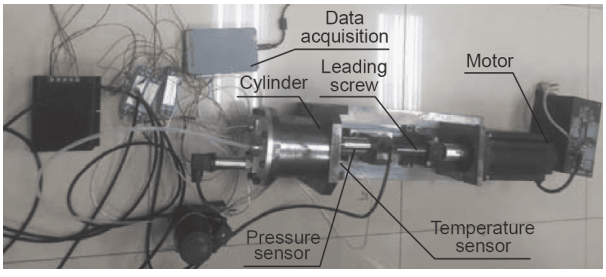

Figure 12 SACRC testbed.

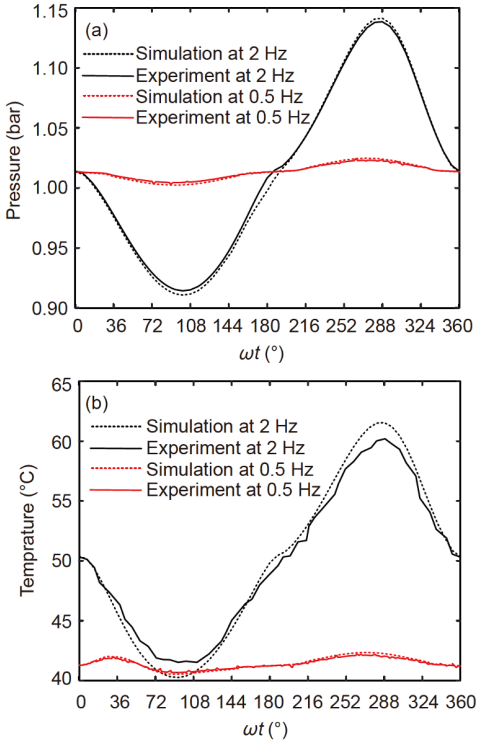

Figure 13 Simulation and experiment curves. (a) Pressure; (b) temperature.

which can miniaturize the high pressure compressor.

(2) The simulation curves agree well with the experiment, which proves the accuracy of model.

(3) The key parameters of the self-air-cooling system are studied and get some conclusions, which is useful for structural design.

1) The hydraulic equivalent diameter of the spiral groove is sensitive to the cooling system especially smaller values.

2) The optimum hydraulic equivalent diameter of the spiral groove is larger with the increasing frequency.

3) The optimum frequency is determined according to the specific conditions.

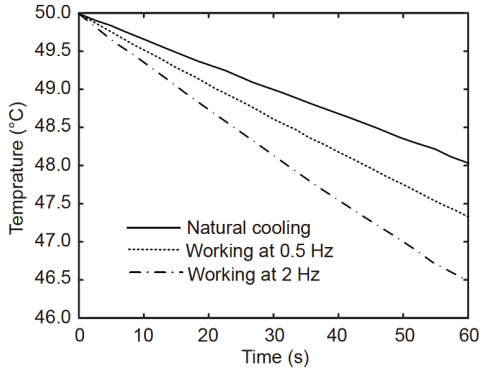

Figure 14 Cylinder temperature.

4) Although the larger or smaller l_p/d can reduce cooling effect, it is insensitive.

This work was supported by the China Postdoctoral Science Foundation (Grant No. 2018M631299) and the National Natural Science Foundation of China (Grant No. 11872006).

1 Luo Y, Wang X. Exergy analysis on throttle reduction efficiency based on real gas equations. Energy, 2010, 35: 181–187
2 Liu H, Zhou J, Zhang S W. Current situation and trend of air-to-air missile launch technology. Aeron Eng Prog, 2018, 9: 147–158
3 Wang S Y. Application of cryocoolers in missile systems. Infrared Tech, 2005, 27: 399–402
4 Liu Y, Miao N, Deng Y, et al. Efficiency evaluation of a miniature multi-stage compressor under insufficient inter-stage cooling conditions. Int J Refrigeration, 2019, 97: 169–179
5 Zhang L, Li S S, Liang Z. Efficiency evaluation and experiment of natural gas reciprocating compressor. J Eng Res, 2017, 5: 170–186, https://kuwaitjournals.org/jer/index.php/JER/article/view/1509
6 Almasi A. Optimum selection and design of reciprocating compressor for petroleum services. Proc Institution Mech Engineers Part E-J Process Mech Eng, 2010, 224: 63–66
7 Willich C, White A J. Heat transfer losses in reciprocating compressors with valve actuation for energy storage applications. J Energy Storage, 2017, 14: 322–328
8 Mascarenhas J S, Chowdhury H, Thirugnanasambandam M, et al. Energy, exergy, sustainability, and emission analysis of industrial air compressors. J Cleaner Production, 2019, 231: 183–195
9 Cullen J M, Allwood J M. Theoretical efficiency limits for energy conversion devices. Energy, 2010, 35: 2059–2069
10 Wang G P, Xu J, Wang B Y. Reason analysis of the excessive high temperature of discharge in piston compressor. Fault Analy, 2017, 6: 51–64
11 Rodrigo K, Jader R B, Cesar J D. Cooling of a reciprocating compressor through oil atomization in the cylinder. In: International Compressor Engineering Conference. Purdue, 2010, 1291: 1–8
12 Francesco B, Giovanni F, Alberto B. Reciprocating compressor cylinder's cooling: a numerical approach using CFD with conjugate heat transfer. In: Proceedings of the ASME 2014 Pressure Vessels & Piping Conference. Anaheim, 2014. 1–10
13 Jia G W, Cai M L, Xu W Q, et al. Energy conversion characteristics of reciprocating piston quasi-isothermal compression systems using water sprays. Sci China Technol Sci, 2018, 61: 285–298
14 Xu X, Hwang Y, Radermacher R. Refrigerant injection for heat pumping/air conditioning systems: literature review and challenges discussions. Int J Refrigeration, 2011, 34: 402–415
15 Zhu Y F. Development of reciprocating air-cool oilless compressors series product. AMR, 2011, 201-203: 1429–1432
16 Deng Y, Miao N, Liu Y, et al. Investigation on cooling efficiency of a 3D-printed integrated inter cooler applicable to a miniature multi-stage compressor. Int J Refrigeration, 2019, 100: 295–306
17 Zhao Y, Feng J, Zhou Q, et al. Blade fracture analysis of a motor cooling fan in a high-speed reciprocating compressor package. Eng Failure Anal, 2018, 89: 88–99
18 Van de Ven J D, Li P Y. Liquid piston gas compression. Appl Energy, 2009, 86: 2183–2191
19 Yan B, Wieberdink J, Shirazi F, et al. Experimental study of heat transfer enhancement in a liquid piston compressor/expander using porous media inserts. Appl Energy, 2015, 154: 40–50
20 0 Yusha V L, Den′gin V G, Busarov S S. The estimation of thermal conditions of highly-cooled long-stroke stages in reciprocating compressors. In: International Conference on Oil and Gas Engineering. Paris, 2015, 113: 264–269
21 Klotsche K, Thomas C, Hesse U. Thermal and fluid mechanical investigation of an internally cooled piston rod. In: The 10th International Conference on Compressors and their Systems. London, 2017, 232: 1–10
22 Heidari M, Mortazavi M, Rufer A. Design, modeling and experimental validation of a novel finned reciprocating compressor for isothermal compressed air energy storage applications. Energy, 2017, 140: 1252–1266
23 Zheng H F. Thermodynamics and the basis of heat transfer (in Chinese). Beijing: Science Press, 2017
24 Cengel Y A. Heat transfer: a practical approach. Boston: McGraw-Hill, 1998